

Evolution of Tidally Truncated Globular Clusters with Anisotropy

Koji Takahashi¹, Hyung Mok Lee² and Shogo Inagaki³

¹Department of Earth and Space Science, Graduate School of Science, Osaka University, Osaka
560, Japan

E-mail: takahasi@vega.ess.sci.osaka-u.ac.jp

² Department of Earth Sciences, Pusan National University, Pusan 609-735, Korea

E-mail: hmlee@uju.es.pusan.ac.kr

³ Department of Astronomy, Kyoto University, Kyoto 606-01, Japan

E-mail: inagaki@kusaastro.kyoto-u.ac.jp

ABSTRACT

The evolution of tidally truncated globular clusters is investigated by integrating two-dimensional Fokker-Planck equation that allows the development of velocity anisotropy. We start from the isotropic Plummer model with tidal cut off and follow the evolution through the core collapse. The heating by three-body binary is included to obtain the evolution past the core collapse. The radial anisotropy in velocity dispersion develops during the pre-collapse evolution in the outer parts of the cluster. However, the anisotropy becomes highly depressed during the post-collapse evolution because of rapid loss of radial orbits. Maximum radial anisotropy appears just after the beginning of the expansion, and degree of anisotropy decreases slowly as the total mass of the cluster decreases. The density profiles of pre-collapse and early phase of post-collapse clusters require King-Michie models while the late phase of clusters can be well represented by isotropic King models. However, the detailed radial behavior of degree of anisotropy of our Fokker-Planck model is somewhat different from that of best-fitting King-Michie models.

Subject headings: Clusters: globular - dynamics

1. INTRODUCTION

Radial velocity anisotropy develops rapidly as a result of two-body relaxation in stellar systems (e.g., Spitzer 1987). It has been well known that highly anisotropic clusters would show $r^{-3.5}$ density profile in the outer parts if the cluster is *isolated* (see, e.g. Binney & Tremaine 1987, p522). The existence of tidal truncation makes the surface density profile more complicated than the simple power-laws. In order to determine the velocity anisotropy, one needs to measure both tangential and radial velocities of large number of stars in a cluster. Detailed studies of globular clusters reveal that some clusters require significant degree of radial anisotropy (e.g., Lupton,

Gunn & Griffin 1985) but many can be fitted by simple King models which have isotropic velocity distribution throughout the clusters (e.g., King 1985).

The dynamical evolution of globular clusters has been investigated intensively in recent years with various numerical techniques. Recent studies on dynamical evolution of globular clusters have focused on the physical processes in the central parts of the clusters where the anisotropy is rather unimportant. The most popular tool of the study of cluster evolution has been the numerical integration of Fokker-Planck equation. Although Cohn (1979) has pioneered the integration of two-dimensional Fokker-Planck equation in energy (E) and angular momentum (J) space, difficulties in obtaining accurate results prevented further use of the two-dimensional Fokker-Planck equation. Instead, one-dimensional isotropic Fokker-Planck equation has been widely used because it is much easier and faster to integrate.

Most of these difficulties have been lifted by adopting more accurate schemes for the integration of two-dimensional Fokker-Planck equation (e.g., Takahashi 1995). These new schemes have been successfully applied to pre-collapse (Takahashi 1995) and post-collapse evolution (Takahashi 1996) of isolated globular clusters. As expected from simple theory as well as gas-dynamical models (e.g., Spurzem 1996), radial anisotropy becomes significant as the cluster experiences the dynamical evolution.

A natural extension of the two-dimensional Fokker-Planck technique is to study the evolution of tidally limited clusters. Here we report the results of such simulations for single component models. In the immediately following section, we describe our models in detail. The results of our numerical integrations are presented in §3. The final section summarizes our findings.

2. Description of Models

We assume only a single mass component in order to maintain the simplicity for the models. The tidal field experienced by the cluster depends on the location of the cluster in the Galaxy. However, we assume that the tidal field is fixed. Thus the cluster is assumed to move along a circular orbit in the spherically symmetric potential. This is clearly unrealistic because the cluster orbit is neither circular nor the Galactic potential is spherically symmetric. The time dependent tidal boundary will affect the rate of evaporation, but qualitative results will be somewhat insensitive to this simplifying assumption. The disk or bulge of the Galaxy could also cause gravitational shock which is very efficient in dissolving the globular clusters (e.g., Gnedin & Ostriker 1997). The effects of tidal shock will be considered in the forthcoming papers.

The tidal boundary is treated as follows. For a star having energy E and angular momentum J , we can determine the apocenter r_a via

$$J^2 = 2r_a^2 [\phi(r_a) - E], \tag{1}$$

where $\phi(r)$ is the gravitational potential. (In this paper we adopt the sign convention for the potential such that $\phi > 0$ inside the cluster.) We have assumed that the star will be lost if the r_a is greater than the tidal radius r_t . The tidal radius is determined by the following condition (e.g., Spitzer 1987),

$$r_t = R_G \left(\frac{3M_C}{M_G} \right)^{1/3}, \quad (2)$$

where R_G is the Galactocentric radius of the orbit, and M_C and M_G are the masses of the cluster and the Galaxy (within radius R_G), respectively.

The removal of stars whose $r_a > r_t$ effectively removes those in radial orbits. We have shown this criteria in (E, J) space for the case of $\phi(r)$ equals to that of Plummer model in Figure 1. Clearly, the stars with low J are preferentially removed and the velocity distribution becomes isotropic. We call this criteria for the evaporation as ‘apocenter condition’.

In order to test the sensitivity of the results on the assumption of tidal evaporation, we also made a separate assumption for the evaporation based on energy constraint: i.e., stars with $E_t = \frac{GM}{r_t} > E$ are assumed to disappear from the cluster. This is essentially the same assumption for the isotropic models considered by Lee & Ostriker (1987) and others. This energy criterion is also shown in Figure 1 as dotted lines. Clearly the difference between these two conditions is somewhat small. For $J = 0$, the apocenter condition becomes identical to the energy condition.

We have included the heating effects by binaries formed via three-body processes. The heating effect is included as an additional term in the Fokker-Planck equation like other calculations (e.g., Cohn 1985; Lee, Fahlman & Richer 1991). The initial cluster is assumed to be the Plummer model with a tidal truncation. Initial tidal radius was set to 32 in Plummer model units. The number of stars in the initial cluster was set to $N = 20000$. This is clearly much smaller than the number of stars in typical clusters. However, the general evolution of the cluster is nearly independent of N except for the central density and core radius. We have chosen such a small N in order to save the computing time: for clusters with larger N the core collapse proceeds to very high central density during which the rest of the cluster remains nearly static. We have employed the direct integration method of Fokker-Planck equation developed by Takahashi (1995).

3. Results

As in the case of isotropic models, the cluster loses only a small fraction of mass until the core collapse. The evaporation becomes important as the cluster begins to expand as a result of binary heating. We now discuss the numerical results of our simulations. For the time being, we will focus on the results obtained using apocenter condition. For the comparison purposes, we also have computed the isotropic models based essentially on Lee, Fahlman & Richer (1991).

3.1. Comparison with Isotropic Models

The evolution of total mass, core, half-mass and tidal radii, and dimensionless evaporation rate ξ as a function of time is shown in Figure 2. The dimensionless evaporation rate ξ is defined as

$$\xi \equiv -\frac{t_{rh}}{M} \frac{dM}{dt}. \quad (3)$$

The time is measured in units of the initial half-mass relaxation time $t_{rh,i}$, and the radii is in Plummer model units. The result for the isotropic model is indicated as a dotted line. The collapse times are $17.5 t_{rh,i}$ and $15.6 t_{rh,i}$ for anisotropic and isotropic models, respectively. The longer duration of core collapse in anisotropic model is probably due to smaller rate of collapse ($t_{rc} d \ln \rho_c / dt$, where t_{rc} is the core relaxation time) for anisotropic models (Louis 1990, Takahashi 1995). The cluster loses mass faster in anisotropic model just after the beginning of the post-collapse expansion. This is due to the fact that the anisotropy builds up at the time of core-collapse. Since the the cluster just after the core collapse has substantial degree of anisotropy, r_h for a similar r_t (or M) cluster is somewhat smaller for anisotropic model than for isotropic model. While the values of ξ are similar for isotropic and anisotropic models, the behavior is somewhat different. In anisotropic model, ξ increases more or less exponentially while the variation is rather mild for isotropic model. The changing degree of anisotropy has clearly played some role here, mainly because of the difference in t_{rh} . In general, we conclude that the global behavior of the total mass and dimensionless evaporation rates are similar between isotropic and anisotropic models.

Ambartsumian (1938) and Spitzer (1940) estimated the evaporation rate for an isolated cluster by assuming that a Maxwellian distribution is established during the relaxation time t_{rh} . The rate ξ is set equal to the fraction of stars that have speeds exceeding the root mean square escape speed $\langle v_e^2 \rangle^{1/2} = 2v_m$, where v_m is the root mean square speed. The Ambartsumian-Spitzer (AS) rate may be modified for a tidally truncated cluster (Spitzer 1987, p57). Using the virial theorem,

$$Mv_m^2 = W \equiv k \frac{GM^2}{r_h}, \quad (4)$$

where W is the total gravitational energy and $k \approx 0.4$ for a wide range of density distribution. The mean square escape speed $\langle v_e^2 \rangle$ in the tidally truncated cluster may be expressed as

$$\langle v_e^2 \rangle = 4v_m^2(1 - \gamma), \quad (5)$$

where

$$\gamma = \frac{1}{2k} \frac{r_h}{r_t}. \quad (6)$$

Thus, the modified AS rate is a function of the ratio of the half-mass radius to the tidal radius, and given by

$$\xi_{AS} = \frac{2}{\sqrt{\pi}} x \exp(-x^2) + \operatorname{erfc}(x), \quad (7)$$

where

$$x = [6(1 - \gamma)]^{1/2}, \quad (8)$$

and erfc is the complementary error function.

Figure 3a shows the evolution of ξ again along with ξ_{AS} for the anisotropic model. In calculating ξ_{AS} we simply set $k = 0.5$, since k is around 0.5 during the post-collapse phase. Note that the results are insensitive to the choice of k . Figure 3b shows the evolution of the ratio r_h/r_t for this model. The behavior of ξ after the core collapse is rather well approximated by ξ_{AS} , i.e., ξ_{AS} increases roughly exponentially. Figures 3a and 3b show that ξ and ξ_{AS} differ by a nearly constant factor of about 2 during the post-collapse phase.

We note here that similar difference between the AS rate and numerical results exists in isotropic clusters. Hénon (1961) found that $\xi = 4.5 \times 10^{-2}$ for his self-similar model for the post-collapse cluster, while ξ_{AS} is estimated to be 2.0×10^{-2} for his model ($r_h/r_t = 0.145$). The reason for having higher values of ξ than ξ_{AS} may be the expansion of the cluster: the stars near the tidal boundary becomes unbound to the cluster as a result of expansion of the cluster. The evaporation rate in an isolated cluster depends somewhat sensitively on the distribution function (e.g., Giersz & Heggie 1994). However, the evaporation rate of the tidally limited cluster is larger than isolated cluster by a large factor. Therefore, we may write $\xi = C\xi_{\text{AS}}$, where C is a numerical factor which may depend on the structure of the cluster and the presence of energy input.

The evaporation rate depends somewhat sensitively on velocity distribution for isolated clusters (e.g., Giersz & Heggie 1994). In our case, we find that ξ for anisotropic cluster varies more significantly than isotropic case. Such a variation can be partially explained by the changes in cluster structure due to the anisotropy. The ratio r_h/r_t increases roughly linearly after the core collapse as shown in Figure 3b. In the right side of equation (7), the first term is dominant for the adequate range of x for the present problem. (If we take $k = 0.5$ and $r_h/r_t = 0.1$, the values of the first and second terms are about 0.012 and 0.0010, respectively.) Therefore, ξ_{AS} increases roughly exponentially with $r_h/r_t \propto t$, unless C changes significantly during the post-collapse evolution. Figures 3c and d are the same as Figures 3a and b, respectively, but for the isotropic model. Also in the isotropic case, the behavior of ξ_{AS} is not far from that of real ξ at the late post-collapse phase. The variation of the ratio r_h/r_t is mild, and the ratio is, roughly speaking, constant throughout almost all of the post-collapse phase. In other words, the post-collapse evolution of the isotropic model is more self-similar than that of the anisotropic model.

The different behavior of ξ between the anisotropic and isotropic models is thus explained, at least in part, by the difference in the evolution of r_h/r_t . Obviously the evolution of the degree of anisotropy has played some role here in making changes to the structure of the cluster. It is still not clear, however, why the ratio increases roughly linearly with time in the anisotropic model.

3.2. Degree of Anisotropy

As we have seen in §2, the degree of anisotropy would be reduced by the presence of the Galactic tidal field because the stars on radial orbits will be preferentially removed from the cluster. This is clearly demonstrated in Figure 4 where the degree of anisotropy as a function of radius is shown at several different epochs. The degree of anisotropy β in this figure is defined as

$$\beta = 1 - \frac{\sigma_t^2}{\sigma_r^2} \quad (9)$$

where σ_t and σ_r are tangential and radial velocity dispersions, respectively. The degree of anisotropy generally increases during the pre-collapse phase, but it decreases as the cluster loses the mass during the post-collapse expansion. Note that the re-expansion starts when the cluster mass becomes about 89% of the initial mass. That epoch is indicated as a solid line in this figure.

The degree of anisotropy increases outward, but reaches maximum at around half of the tidal radius. The peak value of β becomes around 0.6 but decreases rapidly as the cluster loses mass. Just inside the tidal radius, β becomes negative. This is mainly due to the fact that there should be turning points near the tidal radius (e.g., Oh & Lin 1992). Thus the orbit should be predominantly circular near the tidal boundary.

Takahashi (1996) noticed that β reaches around 0.1 for Lagrangian radius of $0.2 M_i$ during the post-collapse phase. Our models with tidal boundary do not show such an asymptotic behavior. The degree of anisotropy clearly gets suppressed by the presence of stellar evaporation.

The degree of anisotropy for the models with *energy condition* are shown in Figure 5. The general behavior is similar to the models with *apocenter condition* except for the outer parts. Instead of having monotonically decreasing behavior after the peak value, β reaches minimum and increases backward. Since energy, or isotropic tidal boundary condition is imposed, β should reach zero at the tidal radius. However, such behavior would not be easily detectable because of extremely low stellar density near the tidal boundary.

The development of negative- β anisotropy at the late evolutionary phase is in part caused by the change of the gravitational potential. (Note that β becomes negative also under the energy condition which does not preferentially remove radial orbits.) The effect of relaxation is relatively weak at this phase because of the low density. The rate of the energy change of a star of energy E and angular momentum J , due to the adiabatic potential change, is given by

$$\frac{dE}{dt} = \int_{r_p}^{r_a} \frac{dr}{v_r} \frac{\partial \phi(r, t)}{\partial t} \bigg/ \int_{r_p}^{r_a} \frac{dr}{v_r}, \quad (10)$$

where $v_r = [2(\phi - E) - J^2/r^2]^{1/2}$. At the late stage of the evolution, $\partial \phi / \partial t$ is negative and increases with r (note $\phi > 0$). Then dE/dt is also negative, and, for halo stars, decreases with J for fixed E . For a halo star, the contribution from the region of $r \approx r_a$ is dominant in the integration in the numerator of equation (10), because the star stays for longer time at this region.

Therefore, dE/dt is more negative for higher J , or smaller r_a . Thus energy E of circular-orbit stars decreases more than that of radial-orbit stars does, and the tangential velocity dispersion exceeds the radial one in the halo.

3.3. Structure of Post-collapse Clusters

Substantial fraction of observed globular clusters have surface brightness distribution close to that of King models. Although the surface brightness distribution is not very sensitive to the velocity anisotropy, highly anisotropic models cannot be fitted to isotropic King models. Here we discuss the structure of post-collapse models with apocenter condition for stellar ejection since the structure of the cluster is not sensitive to the choice of criteria for ejection.

The degree of anisotropy is greatest just before the post-collapse expansion as shown in Figure 4. The total cluster mass in this phase is about 89% of the initial mass. Isotropic King model gives asymptotic slope of -2 in $\log\rho$ versus $\log r$ plot for highly concentrated models, but highly anisotropic pre-collapse cluster has steeper slope. For example, the density profile of the Figure 6 has the slope of -2.45. Thus it is difficult to fit the pre-collapse cluster to an isotropic King model. Instead, we have fitted the density profile of the pre-collapse cluster to a King-Michie model (Fig. 6) with $W_0 = 15$ and $r_{an}/r_c = 300$, where r_{an} is the anisotropic radius. Obviously, King-Michie model gives much better fit than the isotropic King model.

However, the radial profile of degree of anisotropy of our Fokker-Planck model does not match well with that of best-fitting King-Michie model, as shown in Figure 7. The main difference is the presence of plateau of β outside the core radius for the Fokker-Planck result. The penetration of anisotropy to such a small radius was noticed by Louis & Spurzem (1991) and Giersz & Spurzem (1994) using gaseous models and by Takahashi (1995) using Fokker-Planck model. As the core collapse proceeds, the central density-cusp accompanied with constant anisotropy $\beta = 0.08$ extends into the inner region as shown in the above mentioned works. The King-Michie model does not give any such behavior in radial anisotropy profile. The degree of anisotropy of the King-Michie model beyond r_{an} is greater than the Fokker-Planck result. Although the King-Michie models are a convenient representation of stellar systems with radial anisotropy, the runs of anisotropy are significantly different from those produced by dynamical relaxation.

As evident from Figures 4 and 5, the degree of anisotropy decreases as the cluster loses mass. In Figure 8, we have shown the density profiles at $M/M_i = 0.7$ and 0.5. Also shown here are density profiles of isotropic King models having same concentration (dotted lines) as well as best fitting King-Michie models (broken lines). Although the isotropic King models give reasonable fit to our numerical results, the halo is better fitted when small anisotropy is introduced. In fitting to King-Michie models, r_{an}/r_c is not very precisely constrained because the deviation from isotropic King model is rather small.

As the cluster loses significant mass, the clusters become more isotropic. In Figure 9, we

have compared the density profiles at two different epochs ($M/M_i = 0.3$ and 0.12) with the isotropic King models. As in Figure 8, the King models are chosen to have the same concentration parameter $c \equiv \log(r_t/r_c)$. It is clear that the King models can represent the late phase of post-collapse clusters very well. This is simply because the degree of anisotropy is very small during the post-collapse phase. Thus we may conclude that the clusters with less than 50% of the initial mass would have negligible degree of anisotropy.

4. Summary

We have carried out anisotropic Fokker-Planck calculations for the dynamical evolution of globular clusters in static Galactic tidal field. We have considered simple model of single mass component and included the effect of heating by binaries formed by three-body processes in order to obtain the post-collapse evolution. The initial cluster was assumed to be Plummer model with a tidal truncation. As in the case of isotropic cluster models with tidal boundary, the cluster mass decreases roughly linearly in time. Since evaporation time is much larger than the time to core collapse, most mass loss occurs during the post-collapse phase. We have assumed that the stars with apocenter distance greater than the tidal boundary are ejected from the cluster. This ‘apocenter condition’ for the stellar ejection provides preferential removal of stars in radial orbits. We have followed the cluster evolution until the cluster loses about 99% of the initial mass.

The radial anisotropy develops as a result of two-body relaxation in the outer parts. However, we found that the velocity anisotropy in the halo is usually smaller than the isolated models by the presence of Galactic tidal field. During the post-collapse expansion, the degree of anisotropy decreases monotonically with time. The density profiles of clusters in the late phase of post-collapse evolution are found to be well approximated by the isotropic King models because the radial anisotropy is not significant.

In order to find the sensitivity of the results on the assumption of tidal evaporation process, we have also applied different criteria for the stellar ejection: in an alternative model we assumed that the stars are removed from the cluster if $E < E_{tid} = GM/r_t$. This is essentially the same assumption used in isotropic models considered by Lee & Ostriker (1987). This criteria is referred as ‘energy condition’.

The results of ‘energy condition run’ are compared with the apocenter constraint run. The general behavior of the cluster evolution is not much different between these two different models except for outer parts near the tidal boundary. The degree of anisotropy is similarly depressed due to the presence of tidal boundary although the energy condition does not preferably removes the stars on radial orbits. This is found to be due to the fact that most weakly bound stars susceptible for ejection are on radial orbits. Thus we conclude that the suppression of degree of anisotropy is not mere a consequence of the ‘apocenter’ constraint.

Considering the facts that the cluster mass decreases linearly and the degree of anisotropy

decreases in time during the post-collapse phase, we may judge the evolutionary status of the cluster by measuring the degree of velocity anisotropy. However, we need to extend our models to more realistic models in order to reach more quantitative conclusion. We are planning to study models including tidal shock by disk and bulge and initial mass function.

KT was supported by the Grant-in-Aid for Encouragement of Young Scientists by the Ministry of Education, Science, Sports and Culture of Japan (No. 1338). HML was supported by the KOSEF Grant through Grant No. 95-0702-01-01-3.

REFERENCES

- Ambartsumian, V. A. 1938, Ann. Leningrad State Univ., 22, 19 [English trans. in *Dynamics of Star Clusters*, IAU Symp. No. 113, eds. J. Goodman & P. Hut (Dordrecht, Reidel), p521]
- Binney, J., & Tremaine, S., 1987, *Galactic Dynamics*, (Princeton, Princeton Univ. Press)
- Cohn, H. N., 1979, ApJ, 234, 1036
- Cohn, H. N., 1980, ApJ, 242, 765
- Cohn, H. N., 1985, in *Dynamics of Star Clusters*, IAU Symp. No. 113, eds. J. Goodman & P. Hut, (Dordrecht, Reidel), p161
- Giersz, M., & Heggie, D. C., 1994, MNRAS, 268, 257
- Giersz, M., & Spurzem, R., 1994, MNRAS, 269, 241
- Gnedin, O. & Ostriker, J. P., 1997, ApJ, 474, 223
- Hénon, M. 1961, Ann. Astrophys., 24, 369
- King, I. R., 1985, in *Dynamics of Star Clusters*, IAU Symp. No. 113, eds. J. Goodman & P. Hut, (Dordrecht, Reidel), p1
- Lee, H. M., Fahlman, G., & Richer, 1991, ApJ, 366, 455
- Lee, H. M. & Ostriker, J. P., 1987, ApJ, 322, 123
- Louis, P. D., 1990, MNRAS, 244, 478
- Louis, P. D., & Spurzem, R., 1991, MNRAS, 251, 408
- Lupton, R., Gunn, J. E., & Griffin, R. F., 1984, in *Dynamics of Star Clusters*, IAU Symp. No. 113, eds. J. Goodman & P. Hut, (Dordrecht, Reidel), p19
- Oh, K.-S. & Lin, D. N. C., 1992, ApJ, 386, 519

Spitzer, L. Jr., 1940, MNRAS, 100, 397

Spitzer, L. Jr., 1987, *Dynamical Evolution of Globular Clusters*, (Princeton: Princeton Univ. Press)

Spurzem, R., 1996, in *Dynamical Evolution of Star Clusters*, IAU Symp. No. 174, eds. P. Hut & J. Makino (Kluwer, Dordrecht), p111

Takahashi, K., 1995, PASJ, 47, 561

Takahashi, K., 1996, PASJ, 48, 691

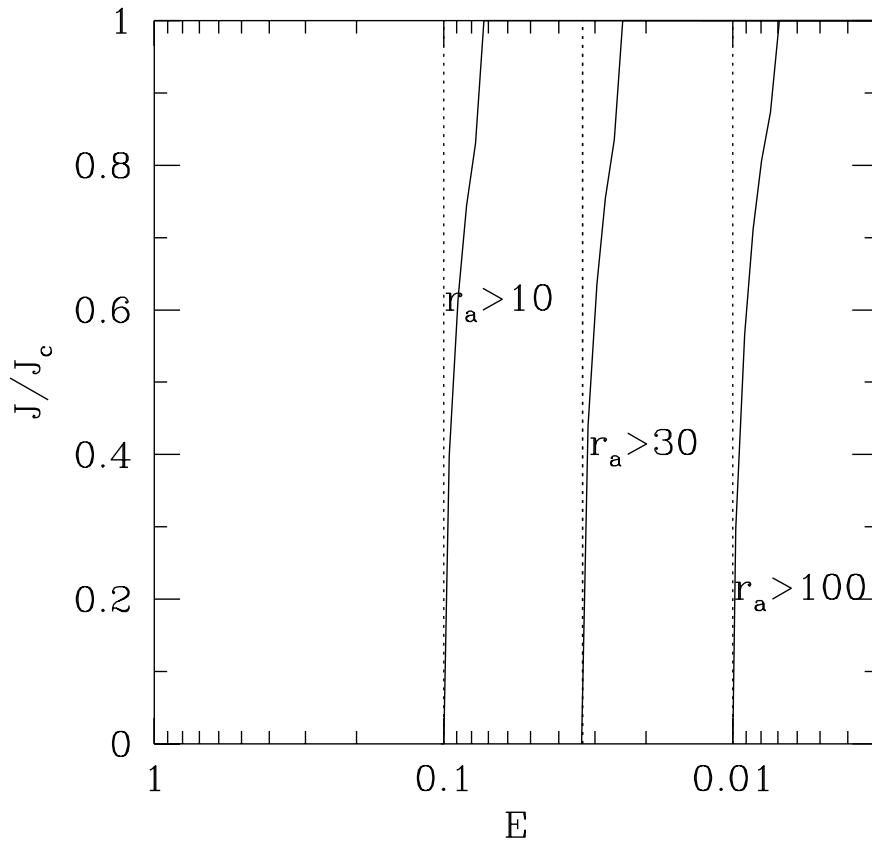


Fig. 1.— The criteria for evaporation of stars in (E, J) space for $r_{tid} = 10, 30$ and 100 . The underlying potential is assumed to be that of a Plummer model and the radius is in Plummer model units. The solid line represents the *apocenter condition* while the dotted line represents the *energy condition*.

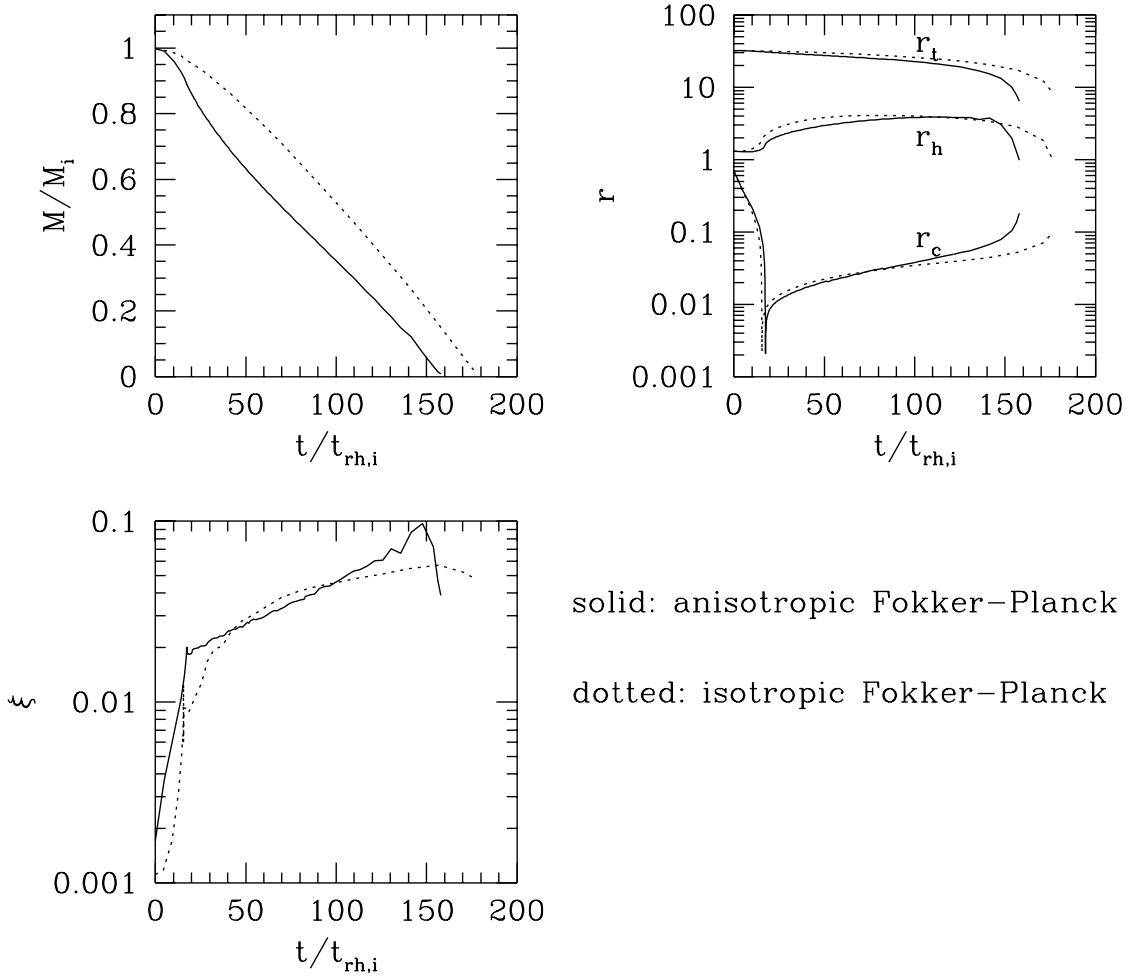


Fig. 2.— Evolution of the (a) total mass, (b) core, half-mass and tidal radii, and (c) ξ as a function of time. The solid line is for the anisotropic result and the dotted line is for the isotropic result.

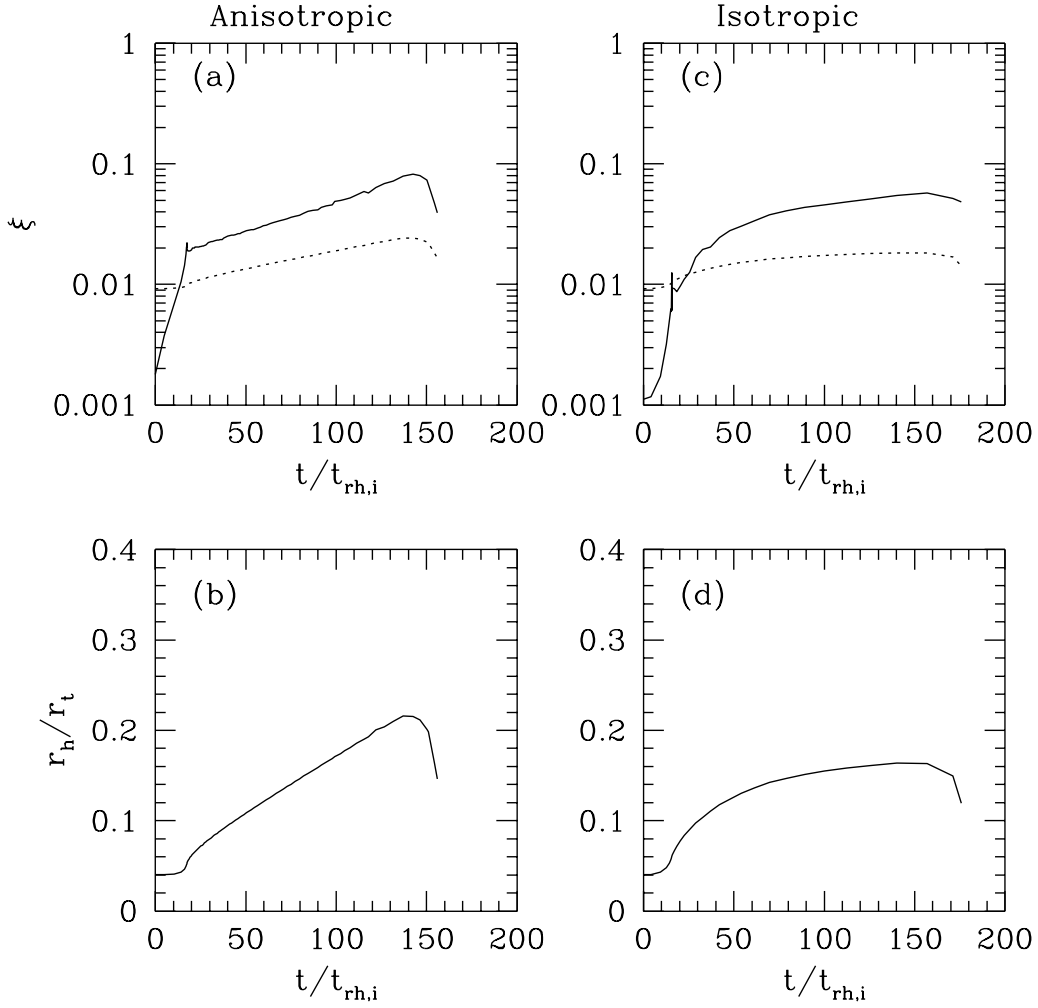


Fig. 3.— Evolution of (a) ξ (solid) and ξ_{AS} (dotted), and (b) r_h/r_t for the apocenter condition anisotropic model. (c), (d) The same as (a) and (b), but for the isotropic model.

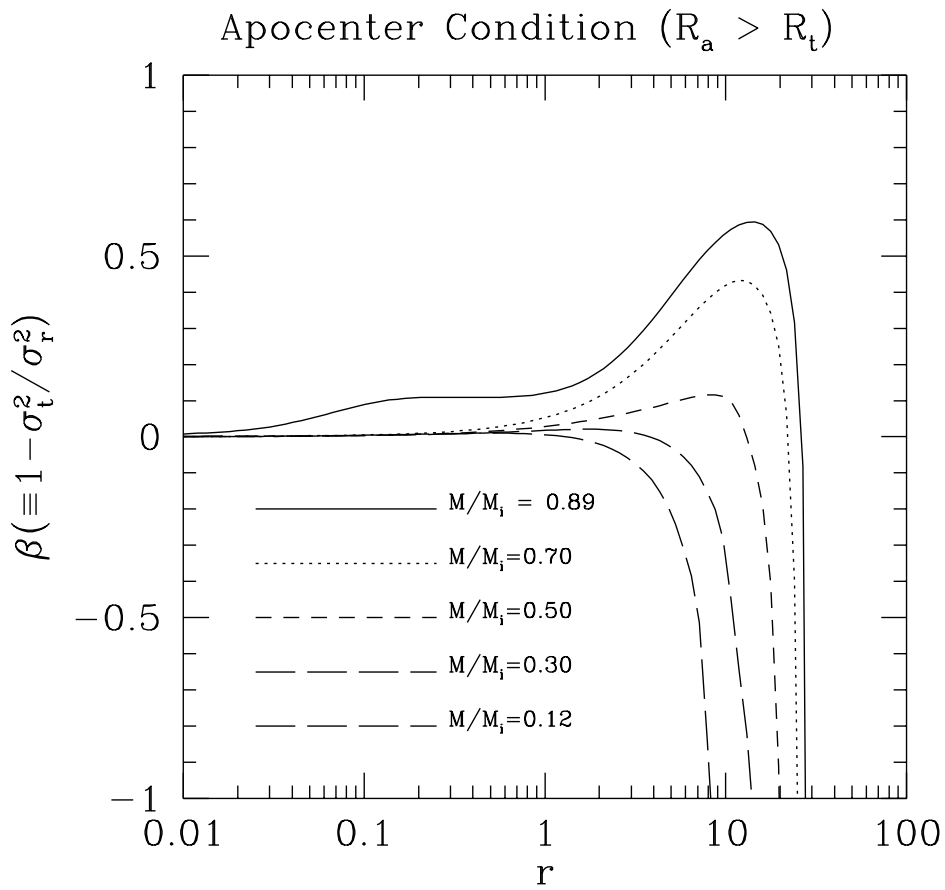


Fig. 4.— The degree of anisotropy as a function of radius for several different epochs for apocenter condition.

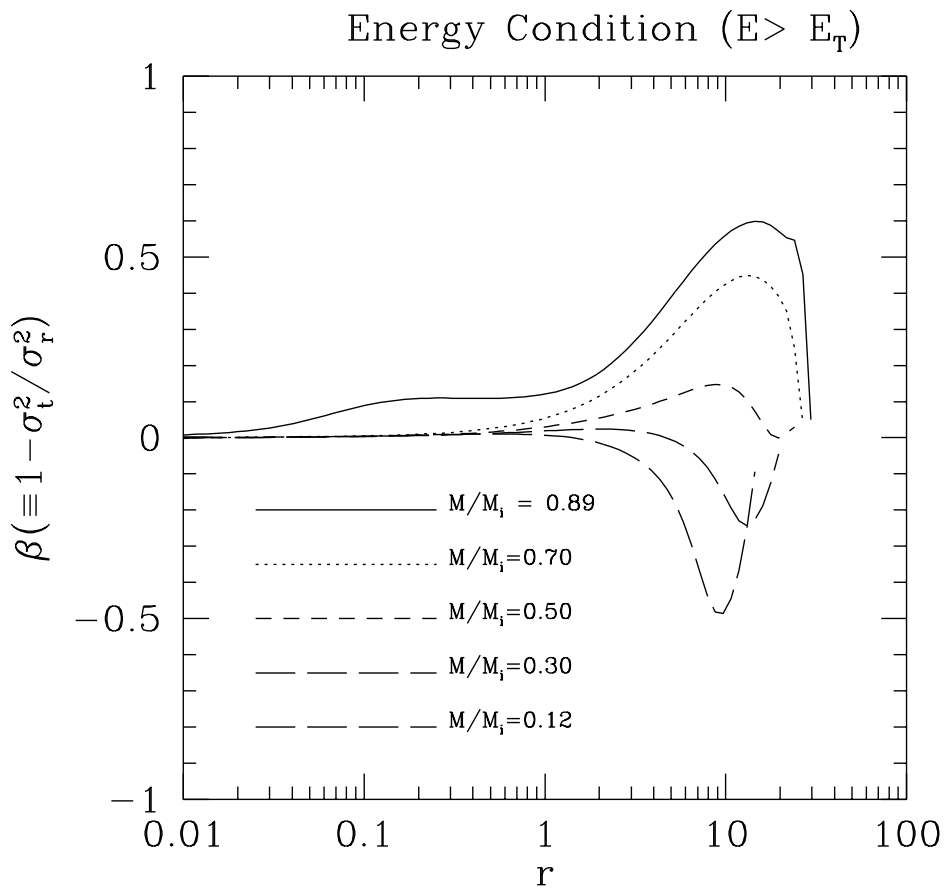


Fig. 5.— Same as Figure 4 except that the energy condition is used for evaporating stars.

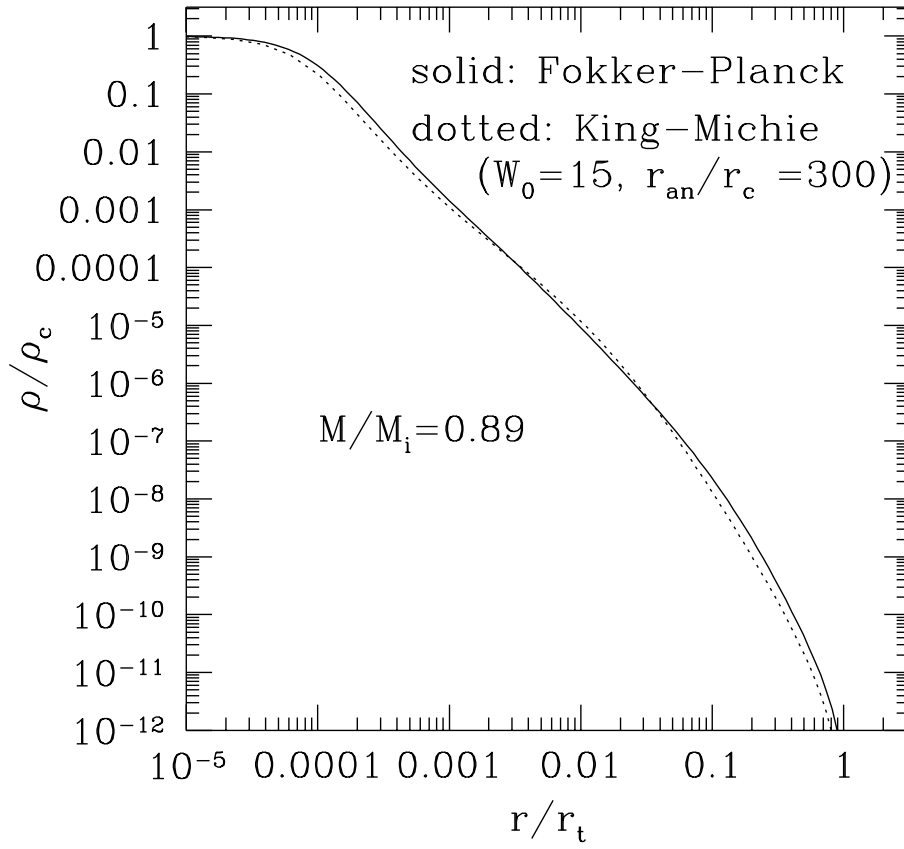


Fig. 6.— The density profile at near the peak core-collapse compared with the best fitting King-Michie model.

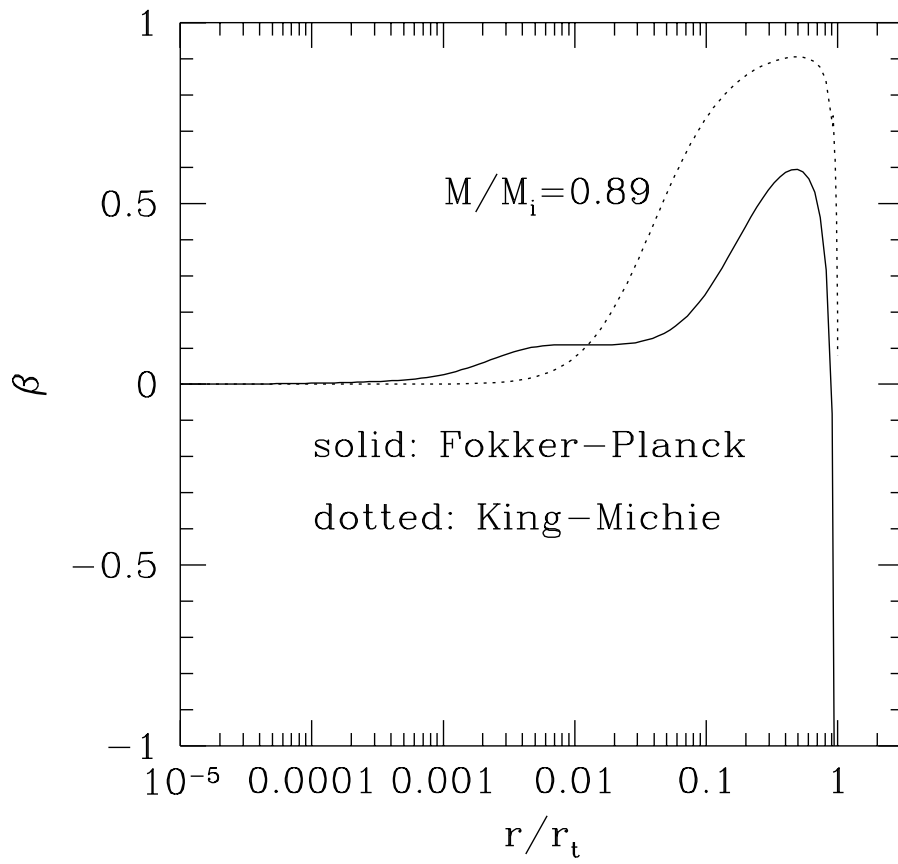


Fig. 7.— Radial distribution of degree of anisotropy for collapsed cluster (solid) and for best-fitting King-Michie model (dotted).

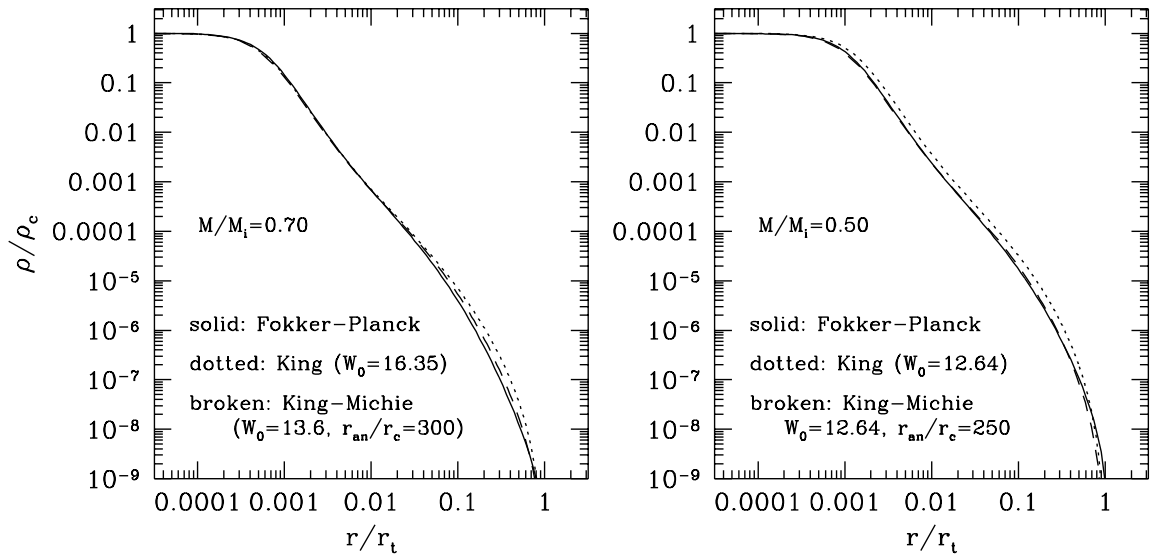


Fig. 8.— The density profiles at two early epochs of post-collapse phase compared with the isotropic King models with the same degree of concentration (dotted lines) and best-fitting King-Michie models (broken lines).

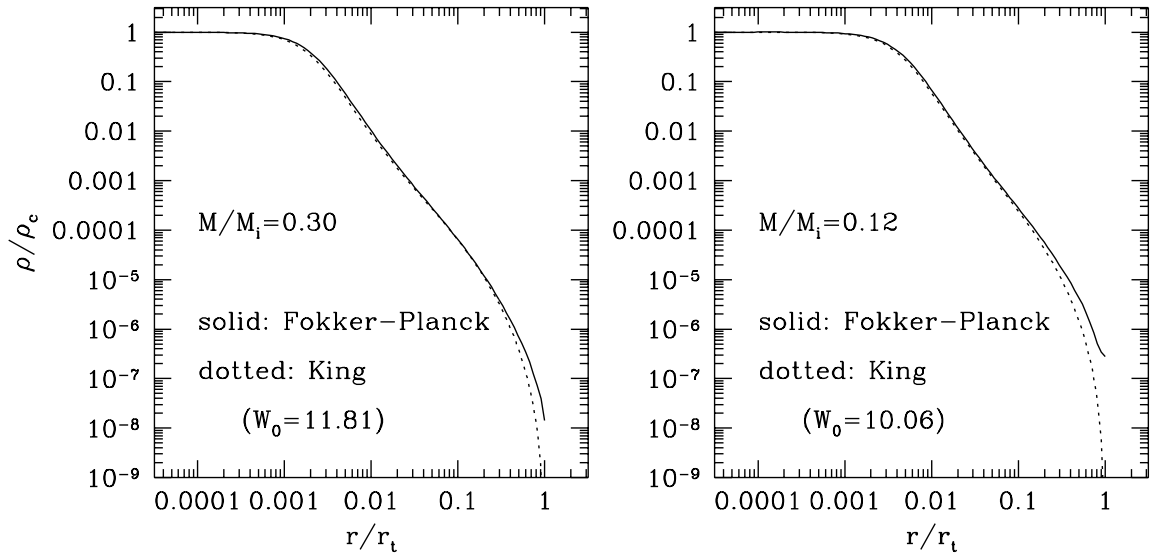


Fig. 9.— The density profiles at two late epochs of post-collapse phase compared with the isotropic King models with the same degree of concentration (dotted lines).